Journal of Molecular Structure 1196 (2019) 707–719

Contents lists available at ScienceDirect

Journal of Molecular Structure

journal homepage: http://www.elsevier.com/locate/molstruc

Sulfonamide-derived hydrazone compounds and their Pd (II) complexes: Synthesis, spectroscopic characterization, X-ray structure determination, in vitro antibacterial activity and computational studies

Neslihan Özbek [a, *], Ümmühan Özmen Özdemir [b], Ahmet Fazıl Altun [b], Ertan Şahin [c]

[a] Department of Mathematics and Science Education, Ahi Evran University, 40100, Kırsehir, Turkey
[b] Department of Chemistry, Faculty of Science, Gazi University, Teknikokullar, Ankara, 06500, Turkey
[c] Department of Chemistry, Faculty of Science, Ataturk University, 25240, Erzurum, Turkey

ARTICLE INFO

Article history:
Received 9 April 2019
Received in revised form
3 July 2019
Accepted 4 July 2019
Available online 5 July 2019

Keywords:
Sulfonamide-derived sulfonyl hydrazones
Pd(II) complexes
Antimicrobial activity
Computational studies

ABSTRACT

A new sulfonamide-derived prophane sulfonyl hydrazone compounds: 2-hydroxy- acetophenoneprophanesulfonylhydrazone (*afpsh*), 5-Cl-2-hydroxyacetophenoneprophane sulfonylhydrazone (*5-Clafpsh*), 3,5-di-tert-butyl-2-hydroxybenzaldehydeprophanesulfonyl hydrazone (*3,5tbsalpsh*) and their Pd(II) complexes were synthesized. The characterization of all compounds was characterized by ^{1}H NMR, ^{13}C NMR, FT-IR, Mass spectral data, elemental analysis and magnetic susceptibility measurements. The crystal structure of *afpsh* was determined by single crystal X-ray diffraction methods. ^{1}H and ^{13}C shielding tensors of *afpsh* were calculated with GIAO/DFT/B3LYP/6–311++G(d,p) methods in DMSO. Molecular electrostatic potential surface and frontier orbital analysis were also carried out. HOMO-LUMO energy gap was calculated which allowed the calculation of relative reactivity descriptors like chemical hardness, chemical inertness, chemical potential, nucleophilicity and electrophilicity index of all compounds. It has been observed that the calculated band gaps for Pd (II) complexes are much smaller than ligands. The microbiological effect of ligands and Pd(II) complexes were tested against six human pathogenic bacteria (three Gram-positive and three Gram-negative strains) by using microdilution (as MICs) and disc diffusion (as mm zone) methods. It was found that all compounds, in particular Pd (II) complexes, were more active than sulfonyl hydrazones.

Published by Elsevier B.V.

1. Introduction

Sulfonamide was first drug to treat bacterial infections. Its discovery in 1932 was the most profound revolution in medicinal chemistry. The invention of sulfonamide triggered the discovery of other anti-bacterial members derived from this chemical group, such as sulfadiazine and sulfadoxine [1]. Sulfonamides have a broad spectrum of antimicrobial activity against a range of bacterial species, both Gram-positive and Gram-negative. Sulfonamide-based molecules are of great importance in the preparation of various biological active compounds [2] as they possess anti convulsant (e.g., topiramate) [3], anti-inflammatory (.eg., valdecoxib) [4] antibacterial [5], antitumor [6], anti-carbonic anhydrase [7], hypoglycemic [8], anti-protease [9] properties. They are also used in the treatment for diabetes (eg acetohexamide) [10].

Sulfonamides are also used in coordination chemistry as ligands in the synthesis of metal complexes with structural [11–13], analytical [14] and biological applications [15–17]. In this regard, a series of sulfonamides have been coordinated and evaluated against cancer [18], tuberculosis [19] and malaria [20]. In 2008, Chohan and Supuran have been synthesized Co(II), Cu(II), Ni (II) and Zn(II) sulfonamide complexes and evaluated their biological activity. These complexes are found to be more active than the free ligands [21]. In recent years, palladium-containing sulfonamides have started to be synthesized and have been investigated antibacterial activity of their complexes. In 1998, Otter et al. described the synthesis of palladium sulfonamide complex, however they were no biological evaluated [22]. Alyar and Adem have reported that Pd(II) complexes containing salicilaldehyde-*N-methyl p*-

* Corresponding author.
E-mail address: nozbek@ahievran.edu.tr (N. Özbek).

https://doi.org/10.1016/j.molstruc.2019.07.016
0022-2860/Published by Elsevier B.V.

toluenesulfonylhydrazone ligand binds and evaluated antibacterial activity [23].

In our previous studies, we synthesized bissulfonamides and tested antibacterial activity [6,24]. We also have reported spectroscopic properties and conformation analysis of aliphatic/aromatic sulfonic acid hydrazide, sulfonic acid 1-methylhydrazide and some sulfonylhydrazone derivatives [25–27], as well as their metal complexes [28,29]. This study describes the synthesis of 2-hydroxyacetophenoneprophanesulfonylhydrazone (*afpsh*),5-Cl-2-hydroxyacetophenoneprophanesulfonylhydrazone (*5-Clafpsh*), 3,5-di-tert-butyl-2-hydroxy benzaldehydeprophanesulfonylhydrazone (*3,5tbsalpsh*) and their Pd(II) complexes, their characterization using elemental analyses, spectrometric methods (FT-IR, ^{1}H –NMR, ^{13}C NMR, LC-MS, UV-Vis), magnetic susceptibility and conductivity measurements and evaluation of their antimicrobial activities. ^{1}H and ^{13}C shielding tensors for crystal structure of ligands were calculated with GIAO/DFT/B3LYP/6–311++G(d,p) methods in DMSO. The frontier molecular orbitals (FMOs) and molecular electrostatic potential maps (MEP) of sulphonyl hydrazine have been investigated by B3LYP/6–311++G(d,p) and B3LYP/LanL2DZ level of theory. The antibacterial activities of all compounds were studied against Gram positive species; *S.aureus* ATCC 25923, *E. faecalis* ATCC 23212, *S. epidermidis* ATCC 34384 and Gram negative species; *K. pneumoniae* ATCC 70063, *P. aeruginosa* ATCC 27853, *E. coli* ATCC 25922 by using microdilution (as MICs) and disc diffusion (as mm zone) methods. Biological studies of Pd(II) complexes with emphasis on its possible application as a novel antibacterial agent are also present in this manuscript.

2. Experimental

2.1. Materials and physical measurements

Propane sulfonyl chloride, hydrazine hydrate, Na_2PdCl_4, 2-hydroxyacetophenone, 5′-chloro-2′-hydroxyacetophenone, 3,5-di-*tert*-butyl-2-hydroxybenzaldehyde, ethanol, methanol, diethyl ether, ethyl acetate, acetonitrile, dimethyl sulfoxide and tetrahydrofuran (all from Sigma-Aldrich) and solvents (all from Merck) were used without further purification. All chemicals and solvents used in synthesis were of analytical grade.

The elemental analyses (C, H, N and S) were performed on a LECO CHNS 9320 type elemental analyzer. ^{1}H -NMR and ^{13}C -NMR spectra were recorded on a Agilent Spectrospin Avance VNMRS -500 Ultra-Shıeld. TMS was used as internal standard and deuteriated DMSO as solvent. The IR spectra (4000-400 cm^{-1}) were recorded on a Mattson 1000 FT-IR Spectrophotometer with samples prepared as KBr pellets. LC/MS-APCI was recorded on an Waters 2695 Alliance Micromass ZQ Spectrometer. The melting points were measured using an Opti Melt apparatus. TLC was conducted on 0.25 mm silica gel plates (60F254, Merck). The molar magnetic susceptibilities were measured on powdered samples using Gouy method. The molar conductance measurements were carried out using a Siemens WPA CM 35 conductometer.

2.2. General procedure for the synthesis of sulfonyl hydrazones

The reaction of the hydrazine hydrate with propane sulfonyl chloride was carried out propane sulfonic acid hydrazide (*psh*) as procedure [30]. The sulfonyl hydrazones were synthesized according to the following general procedure (Fig. 1).

The solution of propane sulfonic acid hydrazide (0.01 mol) in of ethanol was mixed with hot solution of the corresponding aromatic aldehydes (0.015 mol) in ethanol and stirred for 1 h. Upon cooling, crystalline precipitates were filtered, washed with ethanol–ether, recrystallized from water and dried in vacuo over P_2O_5.

2-hydroxyacetophenoneprophanesulfonylhydrazone (*afpsh;* $C_{11}H_{16}N_2SO_3$): Yield 50%; mp:115–116 °C. Elemental analysis: Calcd for C,51.56; H,6.25; N,10.93; S,12.5. Found: C,50.87; H,5.97; N,10.07; S,11.98.

5-chlorine-2-hydroxyaceto phenoneprophanesulfonylhydrazone (*5-Clafpsh;* $C_{11}H_{15}N_2SO_3Cl$): Yield 47%; mp:138–139 °C. Elemental analysis: Calcd for C,45.43; H,5.16; N,9.63; S,11.01. Found: C,45.38; H,5.06; N,9.27; S,10.75.

3,5-di-tert-butyl-2-hydroxybenzaldehydeprophanesulfonylhydrazone (*3,5tbsalpsh;* $C_{18}H_{30}N_2SO_3$): Yield 55%; mp:183–185 °C. Elemental analysis: Calcd for C,61.01; H,8.47; N,7.91; S,9.03. Found: C,60.97; H,7.98; N,7.47; S,9.00.

2.3. Synthesis of the Pd (II) complexes

All complexes are prepared by the following general method (Fig. 1): A sample of anhydrous 0,10 mmol Na_2PdCl_4, was dissolved in acetonitrile (5 mL) and a solution of *afpsh* (0.2 mmol) in a mixture of acetonitrile (10.0 mL) and NaOH solution in methanol (0.2 mmol) was added. The reaction mixture was heated at 60 °C for 1 h. The complexes precipitated quickly after stirring the mixture at room temperature and filtered off, dried in a desiccator over $CaCl_2$.

Pd(afpsh)$_2$ ($C_{22}H_{30}N_4S_2O_6$ Pd): Yield 50%; mp:148–150 °C. Elemental analysis: Calcd for C,42.85; H,4.87; N,9.09; S,10.38. Found: C,41.62; H,4.49; N,8.54; S,10.22.

Pd(5-Clafpsh)$_2$ ($C_{22}H_{28}N_4S_2O_6Cl_2Pd$): Yield 50%; mp:168–170 °C. Elemental analysis: Calcd for C,38.54; H,4.08; N,8.17; S,9.34. Found: C,37.07; H,3.97; N,7.81; S,9.03.

Pd(3,5tbsalpsh)$_2$ ($C_{36}H_{58}N_4S_2O_6$ Pd): Yield 55%; mp:196–198 °C. Elemental analysis: Calcd for C,53.20; H,7.14; N,6.89; S,7.88. Found: C,51.92; H,6.89; N,6.01; S, 7.32.

2.4. Single crystal X-Ray crystallography

For the crystal structure determination, single-crystal of the compound ***afpsh*** was used for data collection on a four-circle Rigaku R-AXIS RAPID-S diffractometer (equipped with a two-dimensional area IP detector). Graphite-monochromated Mo-K_α radiation ($\lambda = 0.71073$ Å) and oscillation scans technique with $\Delta w = 5°$ for one image were used for data collection. The lattice parameters were determined by the least-squares methods on the basis of all reflections with $F^2 > 2\sigma(F^2)$. Integration of the intensities, correction for Lorentz and polarization effects and cell refinement were performed using CrystalClear (Rigaku/MSC Inc.,2005) software [31]. The structure was solved by direct methods using SHELXS-97 [32] and non-hydrogen atoms were refined using anisotropic displacement parameters by full-matrix least-squares procedure using the program SHELXL-97 [32]. H atoms were positioned geometrically and refined using a riding model. The final difference Fourier maps showed no peaks of chemical significance. *Crystal data for* ***afpsh***: $C_{11}H_{16}N_2O_3S$, crystal system, space group: monoclinic, *P*21/a; (no:14); unit cell dimensions: $a = 7.351(2)$, $b = 18.123(5)$, $c = 9.838(4)$ Å, $\alpha = 90$, $\beta = 105.698(6)$, $\gamma = 90°$; volume; 1261.8(7) Å^3, Z = 4; calculated density: 1.35 g/cm^3; absorption coefficient: 0.255 mm^{-1}; *F*(000): 544; θ-range for data collection 2.1–30.7°; refinement method: full matrix least-square on F^2; data/parameters: 3871/161; goodness-of-fit on F^2: 1.023; final *R*-indices [$I > 2\sigma(I)$]: $R_1 = 0.06$, w$R_2 = 0.181$; largest diff. peak and hole: 0.344 and −0.397 e Å^{-3}.

2.5. Theoretical calculations

Because of the effective bioactivities of sulfonyl hydrazine compounds, the three dimensional conformation analysis was

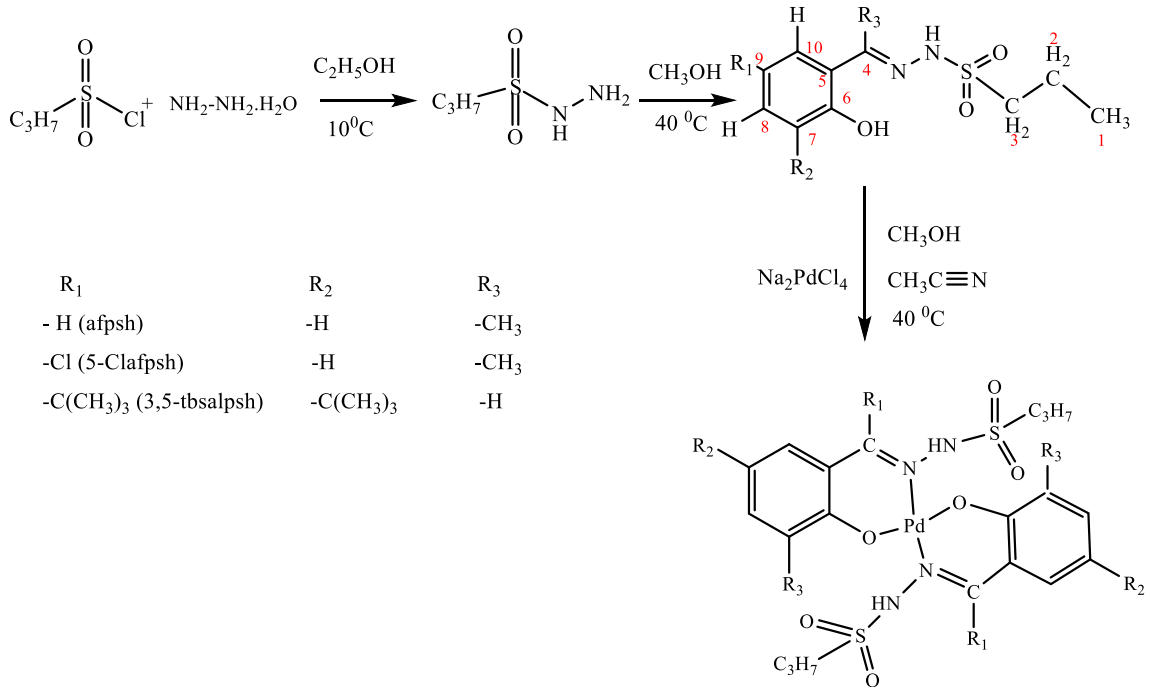

Fig. 1. General synthesis method of the sulfonyl hydrazones and related Pd (II) complexes.

performed to obtain important previews about molecular behavior in gas and solution forms. To determine the most stable structures, all the possible conformations of *5-Clafpsh and 3,5-tbsalpsh* compounds were obtained by potential energy scan. One-dimensional potential energy scans were performed for seven torsion angles- τ1 C8 (H)–C7–N1–N2, τ2 C7–N1–N2–S, τ3 N1–N2–C9–C10, τ4 N2–S–C9–C10, τ5 S–C9–C10–C11, τ6 C10–C9–S–O2 and τ7 N1–N2–S–O2 in the full range of 0–360^0 by DFT method. DFT calculations were performed using Becke's three parameter hybrid exchange functional [33]. B3 combined with both the Lee-Yang-Par gradient-corrected correlation functional (LYP) [34]. In the mentioned conformational analysis of *afpsh*, the molecular geometry optimizations was compared with the Gaussian 03W software package by using DFT approaches in addition to the determination of crystal structure (Fig. 2) [35]. The split valence 6–311++G (d, p) basis set was used for the expansion of the molecular orbital. The ^{1}H and ^{13}C NMR chemical shifts of the compounds were calculated in DMSO using the GIAO method. The geometry optimizations of Pd (II)–sulfonyhydrazone complexes having square planer geometry were applied to confirm the structure as minimum points in energy by B3LYP/LanL2DZ quantum set in Gaussian 09 software program. The ^{1}H and ^{13}C NMR absolute shielding constants were converted to the δ chemical shifts using following equation that σ (TMS) and σ(X_i) are the magnetic shielding constants of reference [36,37] and sample, respectively. NMR calculations were performed in solution phase using the polarizable continuum model (PCM) for DMSO [38]. $\delta_{cal}(Xi) = \sigma(TMS) - \sigma(Xi)$.

In this study, the molecular properties such as ionization potential, electron affinity electronegativity, chemical potential, chemical hardness, softness, electrophilicity index (Equations (1)–(6)) have been deduced from HOMO-LUMO (HOMO-1, HOMO, LUMO, LUMO+1) analysis employing B3LYP/6–311++G(d,p) method. The molecular electrostatic potential maps (MEP) of sulphonyl hydrazine were performed using B3LYP/6–311++G(d,p)

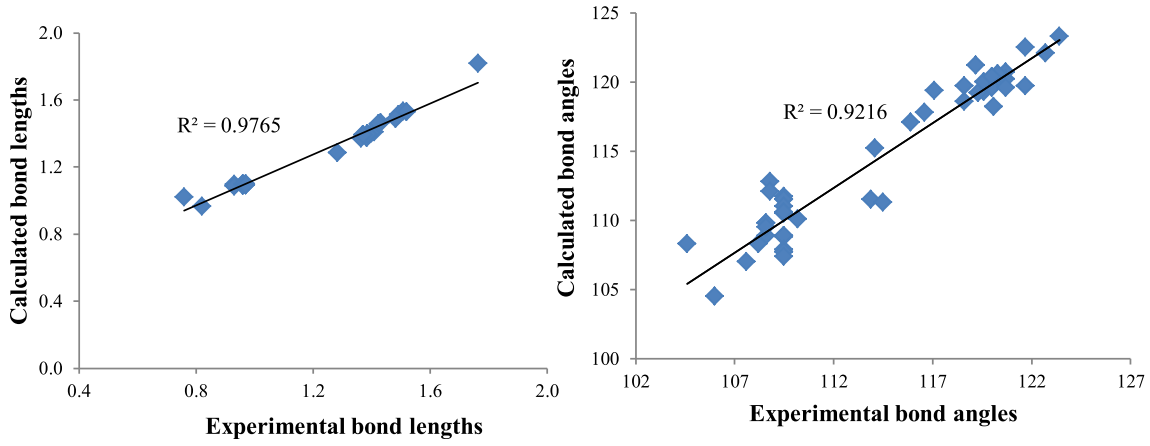

Fig. 2. Bond lengths (Å) and selected bond angles (°) of *afpsh*.

basis set. The MEP surfaces have been mapped with a rainbow color scheme with red representing the highest negative potential region while blue representing the highest positive potential region.

$$\text{Ionization potential(I.P)} = -E_{HOMO}(eV) \quad (1)$$

$$\text{Electron affinity(E.A)} = -E_{LUMO}(eV) \quad (2)$$

$$\text{Electronegativity}(\chi) = (\text{I.P} + \text{E.A})/2(eV) \quad (3)$$

$$\text{Chemical hardness}(\eta) = (\text{I.P} - \chi)/2(eV) \quad (4)$$

$$\text{Softness(s)} = 1/2\eta(eV)^{-1} \quad (5)$$

$$\text{Electrophilicity index}(\psi) = \chi^2/2\eta \quad (6)$$

2.6. Procedure for antibacterial activity

Staphylococcus aureus ATCC 25923, *Enterococcus faecalis* ATCC 23212, *Staphylococcus epidermidis* ATCC 34384, *Klebsiella pneumoniae* ATCC 70063, *Pseudomonos aeruginosa* ATCC 27853, *Escherichia coli* ATCC 25922 cultures were obtained from Gazi University, Department of Biology and bacterial strains were cultured overnight at 310 K in a nutrient broth. During the survey, these stock cultures were stored in the dark at 277 K. The inocula of microorganisms were prepared from broth cultures and suspensions were adjusted to 0,5 McFarland standart turbidity.

The Sulfonamide-derived hydrazones and their Pd(II) complexes were dissolved in dimethylsulfoxide (15% DMSO) to a final concentration of 3.0 mg mL^{-1} and sterilized by filtration with 0,45 μm millipore filters. Antimicrobial tests were then carried out by the disc diffusion method using 100 μL of suspension containing 10^8 CFU mL^{-1} bacteria which was spread on nutrient agar (NA) medium. The discs (6 mm in diameter) were impregnated with 35 μL of each compound (105 μg/disc) at the concentration of 3.0 mg mL^{-1} and placed on the inoculated agar. DMSO impregnated discs were used as negative control. *Sulfisoxazole* (300 μg/disc) were used as positive control to determine the sensitivity of one strain/isolate in each microbial species tested [39]. The inoculated plates were incubated at 37 °C for 24 h for bacterial strains isolates. Antimicrobial activity in the disc diffusion assay was evaluated by measuring the zone of inhibition against the test organisms. Each assay in this experiment was repeated twice. Percentage of inhibition was calculated by comparing the distance of the sample to the distance of *Sulfisoxazole* as standard.

The minimum inhibitory concentration (MIC) values of the sulfonamide derivatives and their complexes were determined using modification of the micro well dilution assay method. 100 μL of the test compounds, initially prepared at 3000 μg mL^{-1} concentration, were added into the first wells. Then, 100 μL of the serial dilutions was transferred into nine consecutive wells. The contents of the wells were mixed and the micro plates were incubated at 37 °C for 24 h. The compounds were tested against each microorganism twice. The values obtained are average of the two results. The MIC values were determined from visual examinations as the lowest concentration of the extracts in the wells with no bacterial growth [40].

3. Results and discussion

We initiated this work by synthesizing a multifunctional prophane sulfonic acid hydrazide (psh) and then synthesized a new sulfonyl hydrazone and their Palladium complexes (Fig. 1). The analytical and spectrophotometric results are consistent with the expected structure of the general formula [ML2].

3.1. Crystal structure of afpsh

Solid-state structure of N'-[1-(2-hydroxyphenyl)ethylidene] propane-1-sulfonohydrazide was confirmed through X-ray diffraction analyses whose molecular diagrams are depicted in Fig. 3a. Molecules of ***afpsh*** form centrosymmetric dimers connected by N2–H···O2 [$D \ldots A = 2.968(3)$Å] hydrogen bonds. There is an intramolecular hydrogen bond between the phenolic OH group and the iminic nitrogen, as evidenced by short O1···N1 distances [d(O···N) = 2.548(3)Å]. Thus, the length of the C1–O1 bond is 1.364 Å, which is consistent with a single bond; while the C1=C7 bond distance is 1.284 Å. The mean plane of the heterocyclic ring is approximately coplanar with the phenyl fragment. The bond lengths between sulphur and oxygen S1–O2 = 1.431(3) Å and S–O3 = 1.423(3) Å falls within the double bond range. The geometry around S atom is significantly deviated from that of regular tetrahedral. The maximum and minimum angles around S are 119.2(3) and 104.5(3), respectively. In all essential details, the geometry of the molecule regarding bond lengths and angles of the compound are in good agreement with the values observed in similar structures [41,42]. Unit cell content with the stacking motif of the molecule is given in Fig. 3b. The list of important bond lengths and bond angles are given in Table 1.

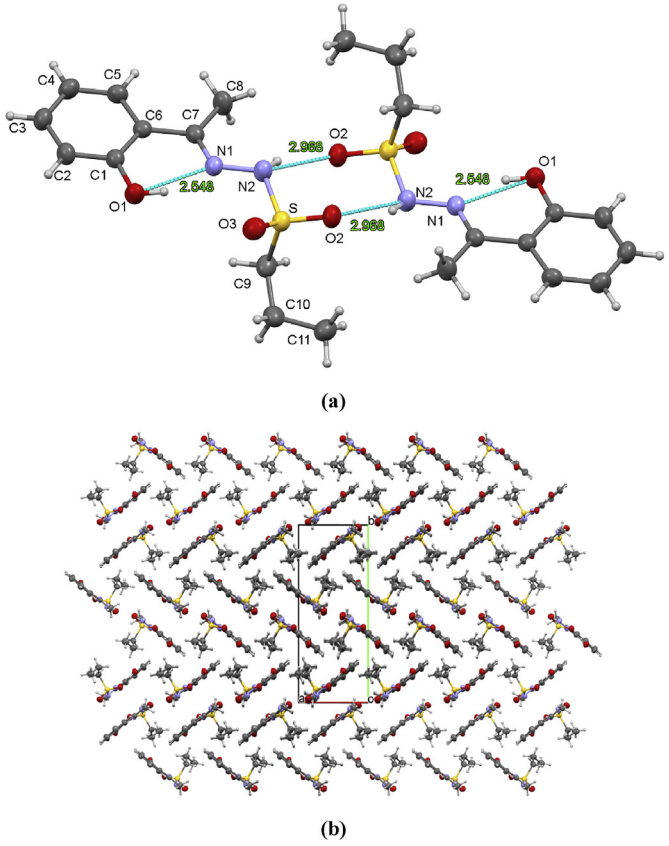

Fig. 3. a) Dimeric structure of the **afpsh** molecule **b)** Unit cell content with the stacking motif of the molecule. Thermal ellipsoids are drawn at the 40% probability level.

Table 1
Selected bond lengths (Å) and bond angles (°) for *afpsh*.

Assig.	Exp.	Calc.	Assig.	Exp	Calc.
The Bond lengths (Å)					
S – O(2)	1.431(2)	1.463	S – O(3)	1.423(2)	1.454
S – C(9)	1.764(3)	1.818	C(3)–C(4)	1.388(5)	1.393
N(2)–N(1)	1.385(4)	1.372	C(9)–C(10)	1.521(5)	1.529
C(1)–C(6)	1.409(4)	1.408	C(1)–C(2)	1.387(4)	1.397
C(7)–C(8)	1.493(4)	1.511	C(6)–C(5)	1.400(4)	1.401
C(5)–C(4)	1.371(5)	1.391	C(2)–C(3)	1.373(5)	1.390
C(3)–H(3)	0.930(3)	1.088	O(1)–C(1)	1.364(4)	1.369
C(11)–C(10)	1.509(6)	1.533	N(1)–C(7)	1.284(4)	1.283
S – N(2)	0.93	1.713	C(7)–C(6)	1.482(4)	1.487
The bond angles (°)					
O(2)-S-O(3)	119,2(2)	121.2	O(2)-S-C(9)	110,2(2)	110.1
O(3)-S-N(2)	107,1(2)	103.1	N(2)-S-C(9)	106,0(2)	104.5
O(1)-C(1)-C(2)	116,2(3)	120.7	O(1)-C(1)-C(6)	123,1(3)	119.1
N(1)-C(7)-C(8)	123,4(3)	123.3	N(1)-C(7)-C(6)	115,9(3)	117.1
C(1)-C(6)-C(5)	116,6(3)	117.8	C(1)-C(6)-C(7)	121,7(3)	122.5
C(6)-C(5)-C(4)	122,7(3)	122.1	C(9)-C(10)-C(11)	114,5(3)	111.3
C(1)-C(2)-C(3)	120,7(3)	120.7	C(5)-C(4)-C(3)	119,3(3)	119.2
C(2)-C(3)-C(4)	119,9(3)	119.9	C(6)-C(7)-C(8)	120,7(3)	119.6
O(2)-S-N(2)	104,6(2)	108.327	C(7)-C(6)-C(5)	121,7(3)	119.7
O(3)-S-C(9)	108,8(2)	108.3	N(2)-N(1)-C(7)	120,1(3)	118.2
S–N(2)-N(1)	114,1(2)	115.2	C(6)-C(1)-C(2)	120,7(3)	120.2
			S–C(9)-C(10)	113,9(3)	111.5

Table 4
The experimental and theoretical ^{1}H and ^{13}C NMR chemical shifts $\delta(ppm)$ for the sulfonylhydrazones.

Assignment	Afpsh		5-Clafpsh		3,5-tbsalpsh	
	Exp.	Calc.	Exp.	Calc.	Exp.	Calc.
C10	128.41	128.2	127.34	127.93	125.96	126.44
C9	118.41	117.8	131.52	139.80	141.36	138.92
C8	125.98	127.9	123.79	125.82	127.49	127.48
C7	117.79	113.0	119.35	110.31	138.99	138.77
C6	153.75	153.5	155.83	155.81	154.49	149.89
C5	125.1	125.8	119.87	119.21	115.99	121.39
C4	156.55	147.6	156.96	149.55	155.15	149.32
C3	53.39	57.3	53.45	56.27	53.04	55.29
C2	14.42	12.4	13.35	13.31	17.10	16.54
C1	11.91	11.82	12.85	12.24	12.88	12.76
R_1 (C–CH_3)	–	–	–		34.10–29.39	35.1–24.88
R_2 (C–CH_3)	–	–	–		35.13–31.40	36.02–29.72
R_3 (CH_3)	.		17.09	10.0	–	
H10	7.3	6.6	7.39	7.44	7.41	7.46
H9	6.8	6.4	–	–	–	–
H8	6.8	6.1	7.25	7.31	7.03	7.23
H7	7.7	6.6	6.92	6.74	–	–
H3	3.19	3.2	3.24	3.26	3.24	3.41
H2	1.75	0.97	1.90	1.71	1.91	1.74
H1	1.02	0.81	1.07	0.92	1.10	0.98
R_1 (CH_3)	–	–	–		1.30	1.14
R_2(CH_3)	–	–	–		1.43	1.33
R_3(CH_3)	2.30	1.9	2.29	2.08	8.07	8.21
OH	11.71	11.27	11.45	10.85	–	
NH	10.61	10.37	–	–	10.47	10.17

σ Transform into using equations given in Ref. [42]; $\delta^{13}C = 175.7–0.963\ \sigma^{13}C$ and $\delta^{1}H = 31.0–0.970\ \sigma^{1}H$.

3.2. The characterization of compounds

3.2.1. Experimental FT-IR spectroscopy

Table 2 shows the assignment of the main bands in the FT-IR spectra of free ligands and complexes, based on some general references and previous studies on complexes with sulfonamides [43]. NH vibrations in ligands are observed between 3177 and 3225 cm^{-1} as strong bands. In the FT-IR spectrum of ligands two bands in the between 1617 and 1622 cm^{-1} and 1500-1540 cm^{-1} regions correspond to the $\upsilon_{(C=N)}$ stretching while in the complexes these bands shifted to lower wavelengths (1583, 1586 and 1611 cm^{-1}, respectively). This behavior, observed in other cases, indicated that the sulfonamide is involved in the coordination [7,44]. On the other hand, the free ligands presented band at between 1248 and 1253 cm^{-1} assigned to υ (C–O) while in the complexes these bands shifted to higher wavenumbers (1270, 1257 and 1251 cm^{-1}, respectively) in accordance with the coordination through this group. This is confirmed by the appearance of the new bands at 548-574 cm^{-1} and 441-466 cm^{-1} due to υ (M – O) and υ (M – N) stretching modes in the Pd(II) complexes respectively. The low-frequency skeletal vibrations due to υ (M – O) and υ (M – N)

Table 2
FT- IR main bands (in cm^{-1}) of sulfonylhydrazones and their Pd(II) complexes.

Ligands/complexes	ν (C=N)	ν(CO)	ν(NH)/δ(NH)	νas (SO_2)/νs (SO_2)	$\nu(CH)_{Ar}$
Afpsh	1622 (m)	1253 (s)	3218 (s)/709 (m)	1330 (s)/1166 (s)	3052 (w) 3024 (w)
Pd(afpsh)$_2$	1583 (m)	1270(s)	3177 (s)/713(m)	1324 (s)/1158 (m)	3033 (w) 3056 (w)
5-Clafpsh	1617 (m)	1251(s)	3216 (s)/760 (m)	1343 (s)/1160 (s)	3048 (w) 2972 (w)
Pd(5-Clafpsh)$_2$	1586 (m)	1257(s)	3130 (s)/743 (m)	1318 (s)/1161 (s)	3051 (m) 2977 (w)
3,5tbsalpsh	1622 (m)	1248(s)	3225 (s)/710 (m)	1311 (s)/1150 (s)	3006 (w) 3041 (w)
Pd(3,5tbsalpsh)$_2$	1611 (m)	1251(s)	3219 (s)/718 (m)	1327 (s)/1158 (s)	3215 (m) 3419 (w)

s = strong, m = medium, w = weak.

Table 3
The mass spectral data of sulfonyl hydrazones and their Pd(II) complexes.

Compounds	Relative intensities of the major ions (*m/z*, %) and assignment
afpsh	$[M+H]^+ = 257.2$ (100%). M–($C_3H_7SO_2$)–C_8H_6N) = 150.0 (47%).
Clafpsh	$[M]^+ = 290.78$ (100%). M – ($C_3H_8SO_2NN$-C_6H_5) = 154.0 (53%).
tbsalpsh	$[M+H]^+ = 355.2$ (100%). M – (C_3H_8S)–C_8H_6N) = 279.0 (22.4%).
Pd(afpsh)$_2$	$[M + Na + CH_3CN]^+$(680.1,%33.94), $[M+Na]^+$(641.1,%100), $[M-2(CH_3)–CH_2–CH_2–CH_3]^+$(540.4,%17,74), [M-L-H]+(359.5, %21,10) [M-2(CH_3)–(CH_2–CH_2–CH_3)–(SO_2–CH_2–CH_2–CH_3)]$^+$ (437.5, %13.94),
Pd(Clafpsh)$_2$	$[M + NH_4]^+$(704.0230,%18.87), [M-(SO2–C_3H_7)–Cl]$^+$(543.1473,%14.54), $[L + Pd+3H]^+$(391.28.41, %9.04), $[L + Pd–C_3H_7]^+$(355.2057,%64.85), [L–(CH_3)–Cl] $^+$(239.2256, %30.90), [L-2(CH_3)–Cl]$^+$(224.0094, %5,5)
Pd(tbsalpsh)$_2$	[M–C_3H_7–2(C(CH_3)$_3$)]+(654, %19,85), [M – C_3H_7–C(CH_3)$_3$)]+(710,%5,03), [M-C(CH_3)$_3$]$^+$ (753, %4.85), [L]$^+$(355, %100), [L- C(CH_3)$_3$–C_2H_5]+(267, %14.91), [L-C_2H_5]$^+$ (324, %9.78), $[L + Pd–C_3H_7]^+$ (416, %14,83).

stretching provided direct evidence for Pd(II) complexations. This behavior agrees with data in the literature [45]. In the spectra of ligands vibrational bands observed 1311-1343 cm^{-1} and 1150-1166 cm^{-1} are assigned to asymmetric and symmetric SO_2 stretching modes, respectively. No shifting of asymmetric and symmetric SO_2 modes in the complexes is attributed to not participating in coordination. This behavior is observed in other compounds [46].

3.2.2. Mass spectra

The mass spectrum of the Sulfonamide-derived hydrazones and Pd(II) complexes is in good agreement with the proposed molecular structure. LC–MS data of aromatic sulfonyl hydrazones and Pd(II) complexes are summarized in Table 3. Mass spectra of *afpsh* gives the molecular ion $[M+H]^+$ peak at *m/z* (intensity %) = 257.2 (100%). By the removal of propane sulfonyl grup ($C_3H_7SO_2$), phenyl amide group is observed at 150.0 (47%). Pd(*afpsh*)$_2$ gives molecular ion,

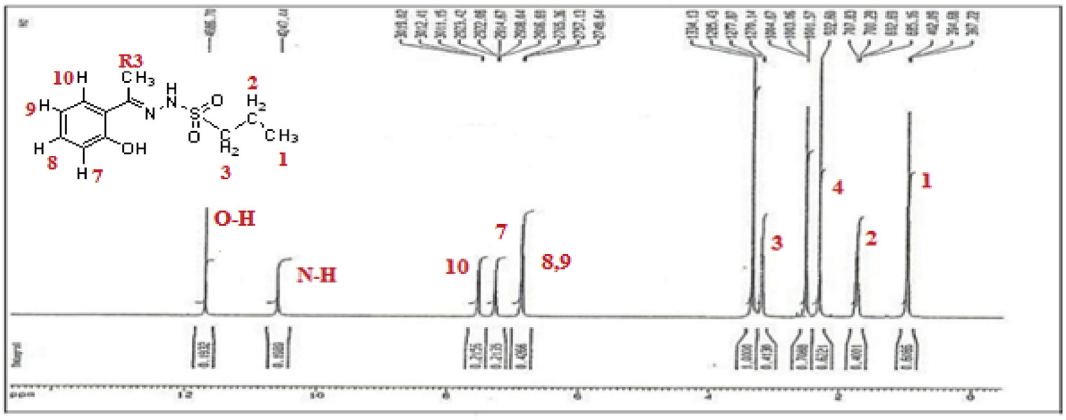

afpsh

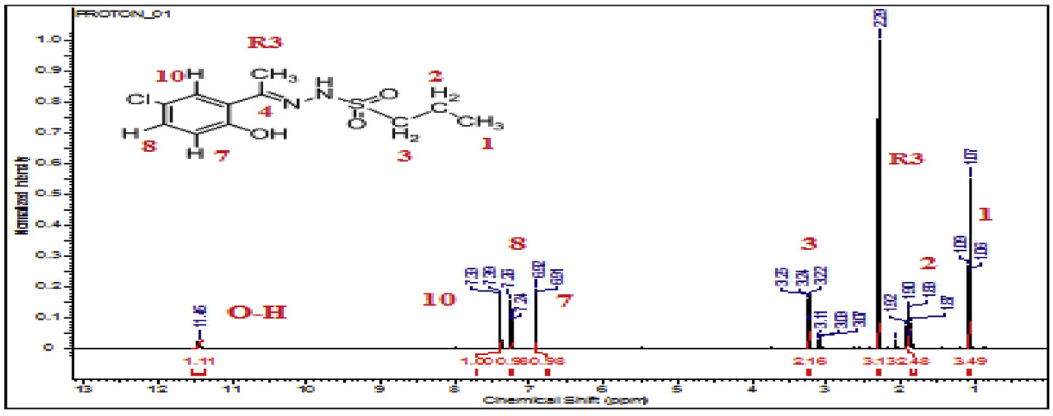

5-Clafpsh

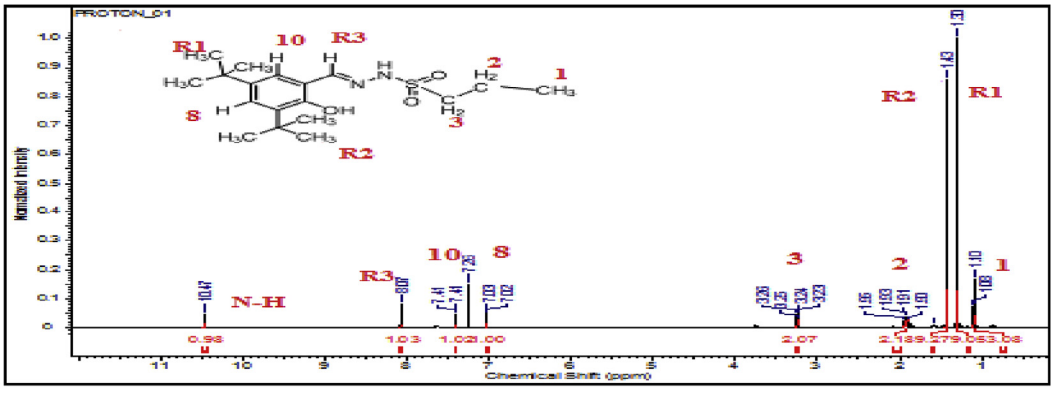

3,5-tbsalpsh

Fig. 4. The experimental ^{1}H NMR spectra of the sulfonylhydrazones.

[Pd(*afpsh*)$_2$ + Na]$^+$ at (641.1, 100%). *Pd(afpsh)$_2$* gives the following fragmentation peaks: 540.4 (17.74%) which occurs by losing of two tert-butyl, 359.5 (21.10%) which occurs by losing of afpsh.

5-Clafpsh gives the molecular ion [M]$^+$ peak at 290.78 (100%). By the removal of propane sulfonyl hydrazine ($C_3H_8SO_2NN$), phenyl group is observed at 154.0 (53%). *Pd(5-Clafpsh)$_2$* gives molecular ion, [Pd(*5-Clafpsh*)$_2$+NH_4]$^+$ at 704.02 (18.87,%). The other fragment with separation of SO_2–C_3H_7–Cl group is observed at 543.15 (14.54%)

3,5-tbsalpsh gives the molecular ion [M+H]$^+$ peak at 355.2 (100%). By the removal of propane sulfonyl (C_3H_8S), phenyl hydrazine group is observed at 279.0 (22.4%). *Pd(3,5tbsalpsh)$_2$* gives the following fragmentation peaks: 654.0 (19.85%) which occurs by losing propyl and two tert-butyl groups, 355.2 (100%) belongs to *3,5-tbsalpsh*.

3.2.3. Electronic spectra and magnetic behavior

The complexes *Pd(afpsh)$_2$*, *Pd(5-Clafpsh)$_2$* and *Pd(3,5tbsalpsh)$_2$* in DMSO solution showed two bands characteristic of square-planar geometry in the 14658-14879 cm^{-1} and 21104-22886 cm^{-1} region assigned to $^1A_{1g} \rightarrow {}^1A_{2g}$ and $^1A_{1g} \rightarrow {}^1B_{1g}$, respectively. The two bands observed in all complexes are assigned to $\pi \rightarrow \pi^*$ transitions of the azomethine (C=N). The magnetic moments of complexes (as B.M) were measured at room temperature. From magnetic measurements, all complexes are founded to be diamagnetic which supports the square planer geometry [12,47].

3.3. Theoretical calculations

3.3.1. Experimental and theoretical ^1H and ^{13}C NMR spectra of afpsh, 5-Clafpsh and 3,5tbsalpsh

Experimental ^1H NMR and ^{13}C NMR spectra of *afpsh, 5-Clafpsh* and *3,5tbsalpsh* were measured and interpreted in DMSO-d_6 solvent. In order to facilitate the interpretation of the NMR spectra, quantum-chemical calculations were performed using B3LYP/6-311G++(d, p) basis set of the compounds in DMSO phase. For the B3LYP/6- 311G++(d, p) method, the chemical shift value tetramethylsilane (TMS) $\delta^{13}C = 175.7 - 0.963\ \sigma^{13}C$ ppm and $\delta^1H = 31.0 - 0.970\ \sigma^1H$ ppm was obtained [42].

The chemical shift values of the compounds are summarized in Table 4. In the ^1H NMR spectra of *afpsh* (Fig. 4), H1, H2 and H3 protons were observed as triplets at 1.02 ppm, 3.19 ppm and

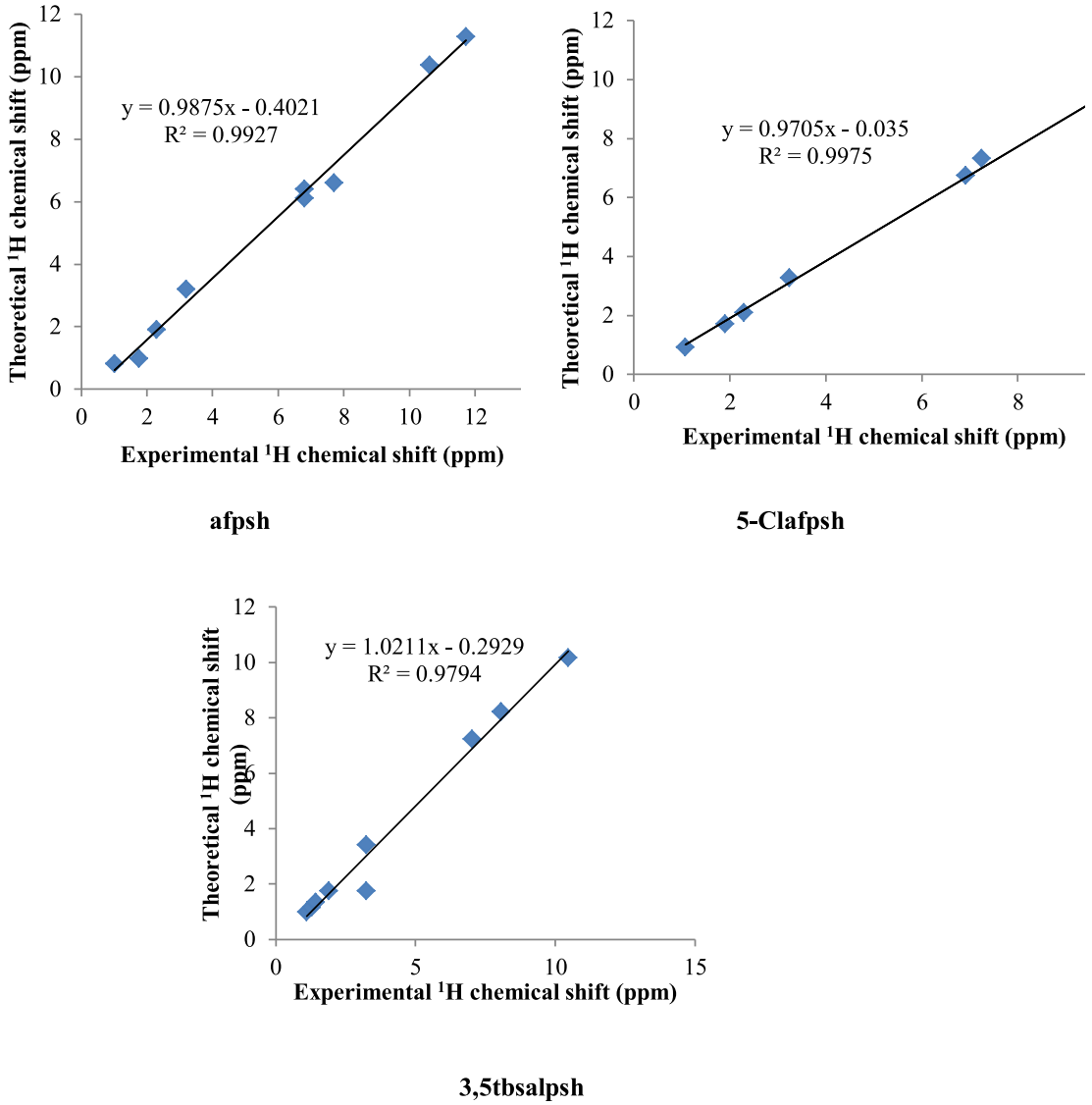

Fig. 5. Plot of the calculated vs. the experimental ^1H NMR chemical shifts $\delta(ppm)$ for the sulfonylhydrazones.

multiplet at 1.75 ppm and calculated values were 0.81 ppm, 0.97 ppm and 3.2 ppm, respectively. Aromatic protons were monitored as doublets at experimentally between 6.8 ppm and 7.3 ppm region and computed were 6.1 ppm and 6.6 ppm, respectively. Experimental and Calculated –NH proton was monitored as singlet at 10.61 ppm and 10.37 ppm. A signal belong to phenolic O–H proton was observed at $\delta = 11.71$ ppm and calculated at 11.27 ppm, respectively. In the ^{1}H NMR spectra of *5-Clafpsh* (Fig. 4), H1, H2 and H3 protons were observed as triplets at 1.07 ppm, 1.90 ppm and multiplet at 3.24 ppm and calculated values were 0.98 ppm, 1.74 ppm and 3.41 ppm, respectively. Aromatic protons were monitored as doublets at experimentally between 6.92 ppm and 7.39 ppm region and computed were 6.74 ppm and 7.44 ppm, respectively. A signal belong to phenolic O–H proton was observed at $\delta = 11.45$ ppm and calculated at 10.85 ppm, respectively. In the ^{1}H NMR spectra of *3,5tbsalpsh* (Fig. 4), H1, H2 and H3 protons were observed as triplets at 1.10 ppm, 1.91 ppm and multiplet at 3.24 ppm and calculated values were 0.92 ppm, 1.74 ppm and 3.41 ppm, respectively. Aromatic protons were monitored as singlet at experimentally between 7.03 ppm and 7.41 ppm region and computed were 7.23 ppm and 7.46 ppm, respectively. Experimental and Calculated –NH proton was monitored as singlet at 10.47 ppm and 10.17 ppm. As seen in Fig. 5, Inclusion of the GIAO model results R^2 values of 0.9927, 0.9975 and 0.9794 and slops of 0.9875, 0.9705, 1.0211 for optimization of all sulfonylhydrazones at the B3LYP/6–311++G(d,p) method.

In ^{13}C NMR spectra of *afpsh*; C1, C2 and C3 carbon signals are assigned at 11.91 ppm, 14.42 ppm and 53.39 ppm (calculated 11.82 ppm, 12.4 ppm and 57.3 ppm) respectively. In ^{13}C NMR spectra of *5-Clafpsh*; C1, C2 and C3 carbon signals are assigned at 12.85 ppm, 13.35 ppm and 53.45 ppm (calculated 12.24 ppm, 13.31 ppm and 56.27 ppm) respectively. Aromatic carbons of *5-Clafpsh* were observed between 119.87 ppm and 131.52 ppm region. In ^{13}C NMR spectra of *3,5tbsalpsh*; C1, C2 and C3 carbon signals are assigned at 12.88 ppm, 17.10 ppm and 53.04 ppm (calculated 12.76 ppm, 16.54 ppm and 55.29 ppm) respectively. Aromatic carbons of *3,5tbsalpsh* were observed between 121.39 ppm and 138.92 ppm region, **-C**H=N- carbon was monitored at 155.15 (experimental) and 149.32 ppm (theoretical). As seen in Fig. 6, Inclusion of the GIAO model results R^2 values of 0.9948, 0.9907 and 0.9934 and slops of 0.9965, 1.0136, 0.9993 for optimization of all sulfonylhydrazones at the B3LYP/6–311++G(d,p) method. These values are very satisfactory at B3LYP/6–311++G(d,p), in general, $R^2 > 0.990$ and slopes which deviate from the ideal values of +1 by no more than 0.05 are indicative of a well performing method. According to results, ^{1}H and ^{13}C NMR chemical shift values show good agreement with experimental ones in Figs. 5 and 6.

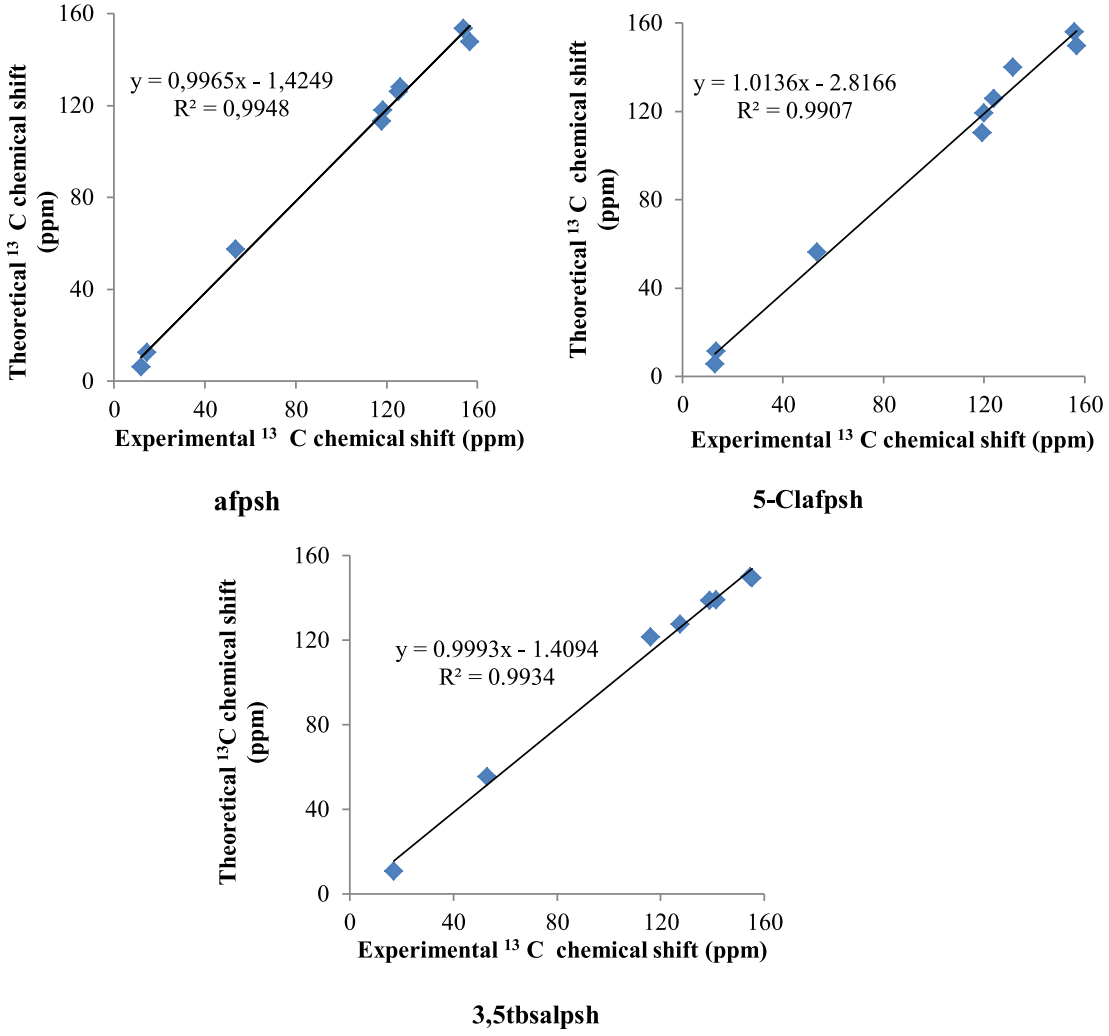

Fig. 6. Plot of the calculated vs. the experimental ^{13}C- NMR chemical shifts *δ(ppm)* for the sulfonylhydrazones.

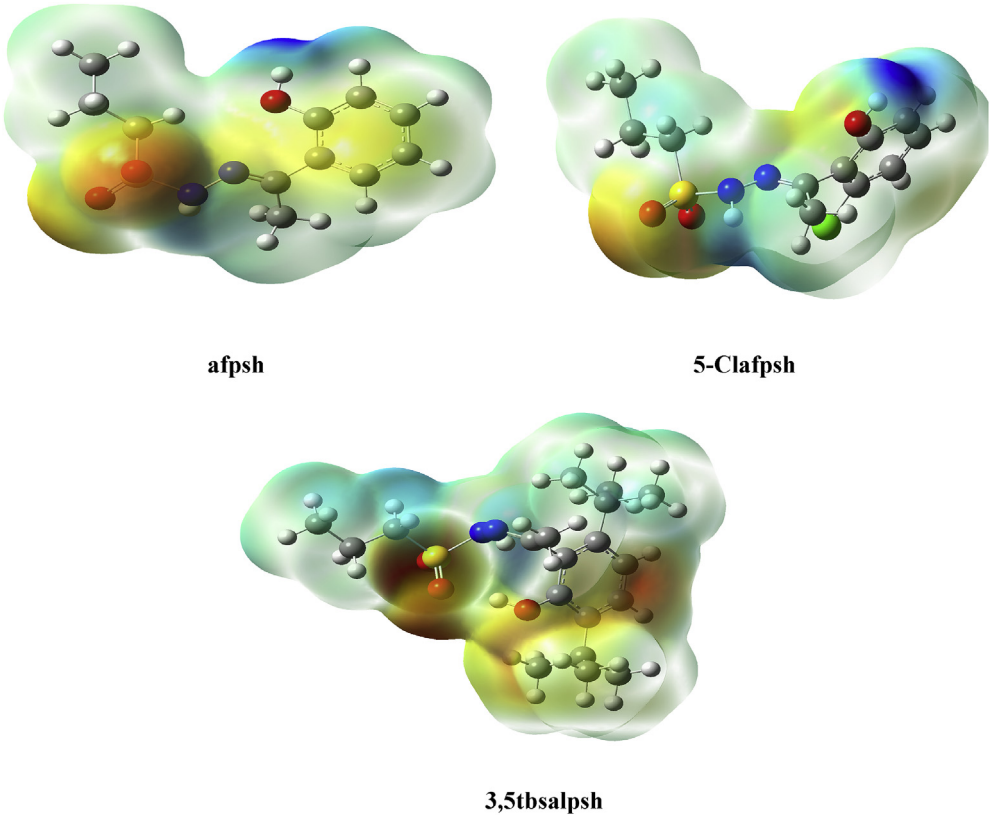

Fig. 7. Molecular electrostatic potential of *afpsh*, *5-Clafpsh* and *3,5tbsalpsh* simulated at B3LYP/6–311++G(d,p).

3.3.2. Molecular electrostatic potential (MEP)

The MEP (*Molecular electrostatic potential)* was related to the electronic density which is a very useful descriptor for determining site for electrophilic attack and nucleophilic reactions. The MEP of the title compounds was optimized geometry using B3LYP method 6–311++G(d,p) was calculated. In Fig. 7, the negative (red) regions of the MEP are related to electrophilic reactivity and positive (blue) regions to nucleophilic reactivity.

As it was seen from Fig. 7, the negative region was distributed on the vicinity of oxygen of SO_2 and the positive regions were localized on nitrogen, hydrogen of N–H group and O–H group, respectively. Therefore, it would be predicted that the oxygen of SO_2 group and nitrogen and hydrogen of amide group and hydroxide group will be more reactive site for both electrophilic and nucleophilic attack [11,48].

3.3.3. Frontier molecular orbital analysis

The Frontier molecular orbitals play an important role in the electric and optical properties, as well as chemical reactions [49].

The highest occupied molecular orbital (HOMO) energies, the lowest unoccupied molecular orbital (LUMO) energies for ligand and three Pd(II) complexes were calculated with B3LYP in 6-311G(d,p) basis set. The results are given in Table 5 and Fig. 8. According to the Koopmans theorem, the energy of the HOMO is related to the ionization potential, while the energy of LUMO is related to the electron affinity [50]. HOMO-1 and LUMO+1,

Table 5
Calculated energies, ionization potential, electron affinity, chemical hardness, softness. Electronegativity, electrophilicity index and dipole moment for sulfonylhydrazones and their Pd(II) complexes.

	TD-DFT/6-311G++(d.p)					
	afpsh	5-Clafpsh	3,5tbsalpsh	Pd(afpsh)$_2$	Pd(5-Clafpsh)$_2$	Pd(3,5tbsalpsh)$_2$
Etotal(Hartree)	−1162.32	−1621.94	−1476.91	−2302.06	−1701.31	−1511.45
E_{HOMO} (eV)	−8.4459	−8.2922	−8.7926	−4.5974	−4.5065	−5.6521
E_{LUMO} (eV)	−5.3106	−4.9723	−5.1005	−4.5571	−4.3590	−5.4122
Δ $E_{HOMO\ -LUMO\ gap}$ (eV)	−3.1353	−3.3199	−3.6921	−0.0403	−0.1475	−0.2399
$E_{HOMO\ -1}$(eV)	−8.5192	−8.5192	−9.4332	−4.7865	−4.5416	−5.7201
$E_{LUMO\ +1}$(eV)	−4.2565	−4.2564	−4.7786	−4.5353	−4.0777	−5.1514
Δ $E_{HOMO\ -1\ -LUMO+1\ gap}$ (eV)	4.2627	4.2628	4.6546	0.2512	0.4939	0.5687
Ionization potential I.P (eV)	8.4459	8.2922	8.7926	4.5974	4.5065	5.6521
Electron affinity E.A (eV)	5.3106	4.9723	5.1005	4.5571	4.3590	5.4122
Electronegativity χ (eV)	6.8783	6.6323	6.9466	4.5773	4.4327	5.5321
Chemical hardness η (eV)	0.7838	0.8299	0.923	0.01005	0.0369	0.0600
Softness (s) $(eV)^{-1}$	0.6379	0.6025	0.5417	49.7513	13.5501	33.333
Electrophilicity index (ψ)	30.1858	26.5016	26.1404	1047.58	266.2443	255.0344
Dipole moment μ (D)	6.9935	6.9556	3.3130	6.1358	5.7198	4.7014

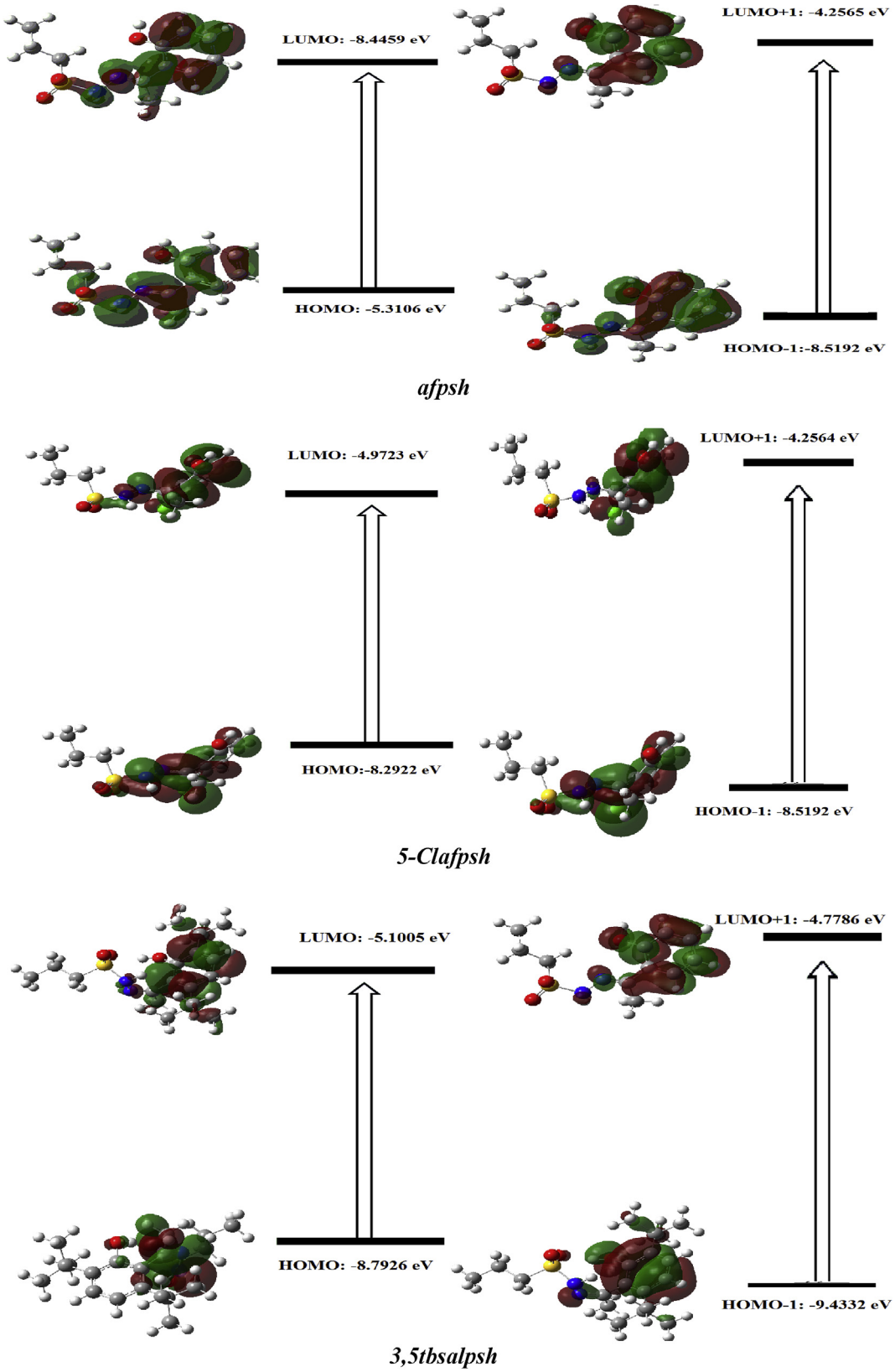

Fig. 8. Plots of the frontier orbitals of the sulfonylhydrazones.

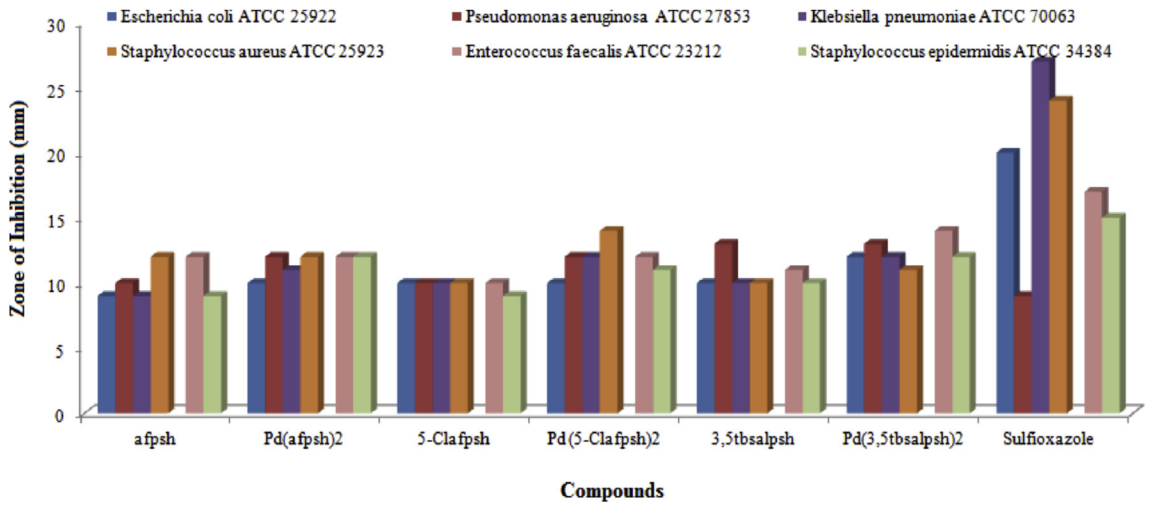

Fig. 9. Measured inhibition zone diameter (mm) of the sulfonylhydrazones, (PdII) complexes and antibiotics by disc diffusion method.

represents one enery state below and above these levels, respectively. The energy gap between HOMO and LUMO is related to the biological activity of the compounds [12,28]. The calculated energies of the HOMO levels for ligands, *afpsh*, *5-Clafpsh* and *3,5tbsalpsh*, show that *5-Clafpsh* has a higher energy of the HOMO (−8.2922 eV) than that of *afpsh* (−8.4459 eV) and *3,5tbsalpsh* (−8.7926 eV). The calculated energy of the LUMO levels for ligands shows that *afpsh* has a lower of the LUMO (−5.3106 eV). Chemical hardness, η, Softness, s, are important properties to measure the molecular stability and reactivity. The calculations indicate that *afpsh* (0.6379 eV) is softer than *5-Clafpsh* (0.6025 eV) and *3,5tbsalpsh* (0.5417 eV), respectively. As shown in Fig. 8 and Table 5, the difference between HOMO and LUMO energy levels of the complexes are 3.2076, 0.1475, 0.0403 eV for *Pd(afpsh)*$_2$, *Pd (5-Clafpsh)*$_2$ and *Pd(3,5tbsalpsh)*$_2$, respectively. The calculated HOMO-LUMO energy gap (ΔE) of the ligands (3.1353, 3.3199 and 3.6921 eV) are lower than that of the palladium (II) complexes (3.2076, 0.1475, 0.0403 eV). The dipole moment is important quantity which reflects the ability of interaction of the molecules with the surrounding environment. The dipole moment of *Pd(3,5tbsalpsh)*$_2$ complex (6.1358 D) is higher than that of *3,5tbsalpsh* (3.3130 D).

3.4. Antibacterial activity results

Sulfonylhydrazones and Pd(II) complexes were investigated for their antibacterial activities against three Gram-positive species (*Staphylococcus epidermidis, Staphylococcus aureus Enterococcus faecalis)* and three Gram-negative species (*Eschericha coli, Pseudomonas aeruginosa, Klebsiella pneumonia)* of bacterial strains by the disc diffusion and micro dilution methods. The antibacterial results were given in Fig. 9 by disc diffusion and Table 6 micro dilution methods. The results were compared with those of the standard drug sulfioxazole (Fig. 10).

The results (Fig. 9) show that *Pd(3,5tbsalpsh)*$_2$ and *Pd(afpsh)*$_2$ have exhibited the strong inhibition effect against most of test bacteria whereas *afpsh* and *3,5tbsalpsh* have weaker activity. All complexes show the highest activities against *P.aeruginosa* which is the mostly effected by *Pd (3,5tbsalpsh)*$_2$ having the diameter zone of 13 mm [28].

Percentage of inhibition for the compounds showed in Fig. 10 that is expressed as excellent activity (120–200% inhibition), good activity (90–100% inhibition), moderate activity (75–85% inhibition), significant activity (50–60%inhibition), negligible activity (20–30% inhibition) and no activity [43]. As seen in Fig. 10, the ligand *3,5tbsalpsh* (144,4%) and *Pd(3,5tbsalpsh)*$_2$ (144.4%), *Pd(afpsh)*$_2$ (133.3%), *Pd (5-Clafpsh)*$_2$ (133.3%) complexes show excellent activity against Gram-negative bacteria *P.aeruginosa*. Also, the compounds exhibit moderate or significant activity against the other tested bacteria (*Sulfisoxazole* is accepted 100% inhibition).

The minimum inhibitory concentration (MIC) was determined for test compounds as well as reference standard in terms of μg/mL and the antimicrobial activity data is summarized in Table 6. According to the MIC's results shown in Table 6, the compounds possess a broad spectrum of activity against the tested bacteria at the concentrations of 93.75–750 μg mL^{-1}. Among the complexes, the *Pd(afpsh)*$_2$ complex has exhibited excellent activity against *P.aeruginosa* strain (MIC 0,304 mM) and its activity is comparable to

Table 6
The MICs of antibacterial activity of the sulfonylhydrazones and their Pd(II) complexes.

Compounds	MIC μg/mL (mM)					
	Gram- negative			Gram-positive		
	E coli ATCC 25922	P.aeruginosa ATCC 27853	K.pneumoniae ATCC 70063	S. aureus ATCC 25923	E.faecalis ATCC 23212	S. epidermidis ATCC 34384
afpsh	375 (**1,46**)	750 (**2,92**)	375 (**1,46**)	375 (**1,46**)	375 (**1,46**)	750 (**2,92**)
Pd(afpsh)$_2$	187,5 (**0,304**)	93.75 (**0.152**)	187,5 (**0,304**)	187,5 (**0,304**)	187,5 (**0,304**)	187,5 (**0,304**)
5-Clafpsh	375 (**1,29**)	750 (**2,58**)	375 (**1,29**)	375 (**1,29**)	375 (**1,29**)	375 (**1,29**)
Pd(5-Clafpsh)$_2$	375 (**0,547**)	375 (**0,547**)	187,5 (**0,273**)	187,5 (**0,273**)	187,5 (**0,273**)	375 (**0,547**)
3,5tbsalpsh	750 (**2,11**)	750 (**2,11**)	750 (**2,11**)	750 (**2,11**)	750 (**2,11**)	>1500 >(**4,22**)
Pd(3,5tbsalpsh)$_2$	375 (**0,461**)	375 (**0,461**)	375 (**0,461**)	375 (**0,461**)	187,5 (**0,231**)	375 (**0,461**)
Sulfisoxazole	23.4 (**0.088**)	375 (**1.403**)	23.4 (**0.088**)	23.4 (**0.088**)	93.75 (**0.35**)	93.75 (**0.35**)

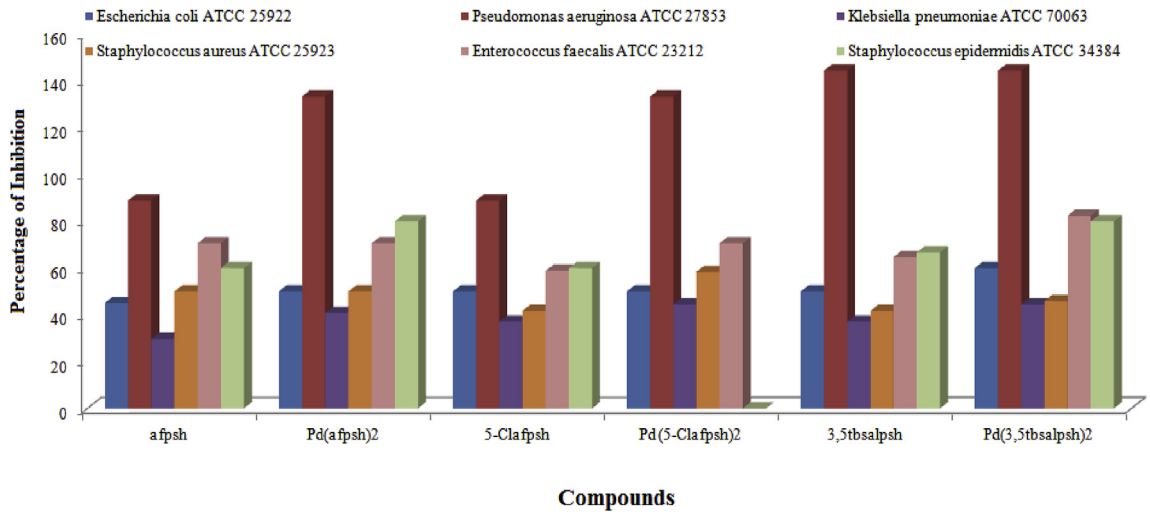

Fig. 10. Percentage of inhibition of the sulfonylhydrazones, (PdII) complexes.

Sulfisoxazole against *E.faecalis* strain (MIC 0,35 mM). Pd(II) complexes are better antibacterial agents than sulfonylhydrazones as expected [51].

4. Conclusion

The experimental and theoretical spectroscopic and electronic properties of three synthesized sulfonamide derivatives, 2-Hydroxyacetophenoneprophanesulfonylhydrazone (*afpsh*), 5-chlorine-2-hydroxyaceto phenoneprophanesulfonylhydrazone (*5-Clafpsh*), and 3,5-Di-tert-butyl-2-hydroxybenzaldehydeprophanesulfonylhydrazone (*3,5tbsalpsh*) were investigated by ^{1}H NMR, ^{13}C NMR, FT-IR, Mass spectroscopies and DFT quantum chemical methods. The crystal structure was determined of *afpsh* by X-ray crystallography. The related palladium (II) complexes of these sulfonamides were obtained and characterized by FT-IR, Mass spectra, elemental analysis and magnetic susceptibility measurements. The theoretical ^{1}H NMR and ^{13}C NMR spectra were compared with the experimental data. Indeed, the calculated chemical shifts were used in the assignment of the studied molecules. Molecular quantities such as ionization potential, electron affinity, electronegativity and chemical hardness, softness, electrophilicity index and dipole moment were calculated and used to predict of the molecules. The computed electronic properties such HOMO, LUMO and HOMO-LUMO energy gaps and molecular electrostatic potential maps predict significant substituent effects of ring activating −NH and −OH groups. The presence of −NH and −OH groups causes a blue shift in the molecular electrostatic potential and decrease in the HOMO-LUMO energy gap in Pd(II) complexes. The antibacterial results showed the palladium (II) complexes to more antibacterial than the sulfonylhydrazone ligands which was as a result of coordination of palladium (II) to the ligands.

As a result, if the MIC values of all compounds are examined, *Pd(afpsh)$_2$* complex shows remarkable activity on six human bacteria than the other compounds. This is probably due to the fact that the Pd complex has lower HOMO− LUMO energy gap ($\Delta E = -0.0403$). The lower LUMO− HOMO energy gap (ΔE) affects the noncovalent binding affinities of the compounds to biological molecules as receptor [52].

Acknowledgement

The authors would like to thank Gazi University BAP (GrantNo: 05/2019-01) for the financial support of this project.

Appendix A. Supplementary data

Crystallographic data that were deposited in CSD under CCDC-1907542 registration number contain the supplementary crystallographic data for this structure (***afpsh***). These data can be obtained free of charge from the Cambridge Crystallographic Data Centre (CCDC) via www.ccdc.cam.ac.uk/data_request/cif and are available free of charge upon request to CCDC, 12 Union Road, Cambridge, UK (fax: +441223 336033, e-mail: deposit@ccdc.cam.ac.uk).

References

[1] G. Domagk, Ein Beitrag zur Chemotherapie der bakteriellen Infektionen, Deut.Med.Wochenschr. 61 (1935) 250–253.
[2] M. Danish, A. Bibi, K. Gilani, M.A. Raza, M. Ashfaq, M.N. Arshad, A.M. Asiri, K. Ayub, Antiradical, antimicrobial and enzyme inhibition evaluation of sulfonamide derived esters; synthesis, X-Ray analysis and DFT studies, J. Mol. Struct. 1175 (2019) 379–388.
[3] T. Tanaka, N. Yajima, T. Kiyoshi, Y. Miura, S. Iwama, N-alkyl-[1,10-biphenyl]-2-sulfonamide derivatives as novel broad spectrum anti-epileptic drugs with efficacy equivalent to that of sodium valproate, Bioorg. Med. Chem. Lett 27 (2017) 4118–4121.
[4] A.A.M. Abdel-Aziz, A. Angeli, A.S. El-Azab, M.E.A. Hammouda, M.A. El-Sherbeny, C.T. Supuran, Synthesis and anti-inflammatory activity of sulfonamides and carboxylates incorporating trimellitimides: dual cyclooxygenase/carbonic anhydrase inhibitory actions, Bioorg. Chem. 84 (2019) 260–268.
[5] N. Özbek, H. Katırcıoğlu, N. Karacan, T. Baykal, Synthesis, characterization and antimicrobial activity of new aliphatic sulfonamide, Bioorg. Med. Chem. 15 (2007) 5105–5109.
[6] A.C. Hangan, G. Borodi, R.L. Stan, E. Pall, M. Cenariu, L.S. Oprean, B. Sevastre, Synthesis, crystal structure, DNA cleavage and antitumor activity of two copper(II) complexes with N-sulfonamide ligand, Inorg. Chim. Acta 482 (2018) 884–893.
[7] S. Alyar, C. Şen, H. Alyar, Ş. Adem, A. Kalkancı, U.O. Özdemir, Synthesis, characterization, antimicrobial activity, carbonic anhydrase enzyme inhibitor effects, and computational studies on new Schiff bases of Sulfa drugs and their Pd(II), Cu(II) complexes, J. Mol. Struct. 1171 (2018) 214–222.
[8] A.E. Boyd, Sulfonylurea receptors, ion channels, and fruit flies, 3rd Diabetes 37 (1988) 847–850.
[9] C.T. Supuran, A. Scozzafava, A. Mastrolorenzo, Bacterial proteases: current therapeutic use and future prospects for the development of new antibiotics, Expert Opin. Ther. Pat. 11 (2001) 221–259.
[10] N. Ghareb, N.M. El-Sayed, R. Abdelhameed, K. Yamada, M.S. Elgawish, Toward a treatment of diabesity: rational design, synthesis and biological evaluation of benzene-sulfonamide derivatives as a new class of PTP-1B inhibitors, Bioorg. Chem. 86 (2019) 322–338.

[11] P. Shafieyoon, E. Mehdipour, Y.S. Mary, Synthesis, characterization and biological investigation of glycinebased sulfonamide derivative and its complex: vibration assignment, HOMO e LUMO analysis, MEP and molecular docking, J. Mol. Struct. 1181 (2019) 244–252.
[12] A. Bouchoucha, S. Zaater, S. Bouacida, H. Merazig, S. Djabba, Synthesis and Characterization of new complexes of nickel (II), palladium (II) and platinum(II) with derived sulfonamide ligand: structure, DFT study, antibacterial and cytotoxicity activities, J. Mol. Struct. 1161 (2018) 345–355.
[13] C.M. Sharaby, M.F. Amine, A.A. Hamed, Synthesis, structure characterization and biological activity of selected metal complexes of sulfonamide Schiff base as a primary ligand and some mixed ligand complexes with glycine as a secondary ligand, J. Mol. Struct. 1134 (2017) 208–216.
[14] R.B. Hoff, G. Rübensam, L. Jank, F. Barreto, M.C.R. Peralba, T.M. Pizzolato, M.S. Diaz –Cruz, D. Barcelo, Analytical quality assurance in veterinary drug residue analysis methods: matrix effects determination and monitoring for sulfonamides analysis, Talanta 132 (2015) 443–450.
[15] A. Ashraf, W.A. Siddiqui, J. Akbar, G. Mustafa, H. Krautscheid, N. Ullah, B. Mirza, M. Hanif, C.G. Hartinger, Metal complexes of benzimidazole derived sulfonamide: synthesis, molecular structures and antimicrobial activity, Inorg. Chim. Acta 443 (2016) 179–185.
[16] Ü.Ö. Özdemir, E. Aktan, F. İlbiz, A.B. Gündüzalp, N. Özbek, M. Sarı, Ö. Çelik, S. Saydam, Characterization, antibacterial, anticarbonic anhydrase II isoenzyme, anticancer, electrochemical and computational studies of sulfonic acid hydrazide derivative and its Cu(II) complex, Inorg. Chim. Acta 423 (2014) 194–203.
[17] S. Alyar, N. Özbek, N.O. İskeleli, N. Karacan, Synthesis, characterization, and antimicrobial activity of copper(II) complexes with N,N0-propanediyl-bis-benzenesulfonamide and N,N'-ethanediyl-bis-2- methylbenzenesulfonamide, Med. Chem. Res. 22 (2013) 2051–2060.
[18] U.O. Ozdemir, N. Özbek, Z.K. Genc, F. İlbiz, A.B. Gündüzalp, New bioactive silver(I) complexes: synthesis, characterization, anticancer, antibacterial and anticarbonic anhydrase II activities, J. Mol. Struct. 1138 (2017) 55–63.
[19] M. Mondelli, F. Pavan, P.C. de Souza, C.Q. Leite, J. Ellena, O.R. Nascimento, G. Facchin, M.H. Torre, Study of a series of cobalt(II) sulfonamide complexes: synthesis, spectroscopic characterization, and microbiological evaluation against M. tuberculosis. Crystal structure of [Co(sulfamethoxazole)2(H2O)2]_H2O, J. Mol. Struct. 1036 (2013) 180–187.
[20] G.M. Fisher, S. Bua, S.D. Prete, M.A.J. Arnold, C. Capasso, C.T. Supuran, K.T. Andrews, S.A. Poulsen, Investigating the antiplasmodial activity of primary sulfonamide compounds identified in open source malaria data, Int. J. Parasitol.: Drugs and Drug Resis. 7 (2017) 61–70.
[21] Z.H. Chohan, C.T. Supuran, Structure and biological properties of first row d-transition metal complexes with N-substituted sulfonamides, J. Enzym. Inhib. Med. Chem. 23 (2008) 240–251.
[22] C.A. Otter, M. Couchman, J.C. Jeffery, K.L.V. Mann, E. Psillakis, M.D. Ward, Complexes of a new bidentate chelating pyridylkulfonamide ligand with copper(II), cobalt(II) and palladium(II) : crystal structures and spectroscopic properties, Inorg. Chim. Acta 278 (1998) 178–184.
[23] S. Alyar, Ş. Adem, Synthesis, characterization, antimicrobial activity and carbonic anhydrase enzyme inhibitor effects of salicilaldehyde-N-methyl p-toluenesulfonylhydrazone and its Palladium(II), Cobalt(II) complexes, Spectrochim. Acta Mol. Biomol. Spectrosc. 131 (2014) 294–302.
[24] S. Alyar, N. Özbek, K. Kuzukıran, N. Karacan, Quantitative structure–activity relationships studies for prediction of antimicrobial activity of synthesized disulfonamide derivatives, Med. Chem. Res. 20 (2011) 175–183.
[25] U. Ozmen Ozdemir, A. Altuntaş, A. Balaban Gündüzalp, F. Arslan, F. Hamurcu, New Aromatic/heteroaromatic propanesulfonylhydrazone compounds: synthesis, physical properties and inhibition studies against carbonic anhydrase II (CAII) enzyme, Spectrochim. Acta, Part A 128 (2014) 452–460.
[26] S. Alyar, H. Alyar, U. Ozmen Ozdemir, O. Sahin, K. Kaya, N. Ozbek, A.B. Gunduzalp, Synthesis, characterization, antibacterial activity and quantum chemical studies of N'-Acetyl propane sulfonic acid hydrazide, J. Mol. Struct. 1094 (2015) 237–245.
[27] U.O. Ozdemir, F. İlbiz, A.B. Gunduzalp, N. Ozbek, Z.K. Genc, F. Hamurcu, S. Tekin, Alkyl sulfonic acide hydrazides: synthesis, characterization, computational studies and anticancer, antibacterial, anticarbonic anhydrase II (hCA II) activities, J. Mol. Struct. 1100 (2015) 464–474.
[28] N. Ozbek, S. Alyar, B.K. Memmi, A.B. Güzndüzalp, Z. Bahçeci, H. Alyar, Synthesis, characterization, computational studies, antimicrobial activities and carbonic anhydrase inhibitor effects of 2-hydroxy acetophenone-N-methyl p-toluenesulfonylhydrazone and its Co(II), Pd(II), Pt(II) complexes, J. Mol. Struct. 1127 (2017) 437–448.
[29] U. Ozdemir, P. Güvenç, E. Şahin, F. Hamurcu, Synthesis, characterization and cobalt(II) complexes, Inorg. Chim. Acta 362 (2009) 2613–2618.
[30] U.O. Ozdemir, G. Olgun, Synthesis, characterization and antibacterial activity of new sulfonyl hydrazone derivatives and their nickel(II) complexes, Spectrochim. Acta, Part A 70 (2008) 641–645.
[31] Rigaku/MSC, Inc., 9009 New Trails Drive, TheWoodlands, TX 77381.
[32] G.M. Sheldrick, Acta Crystallogr. A64 (2008) 112.
[33] A.D. Becke, Density-functional thermochemistry. III. The role of exact exchange, J. Chem. Phys. 98 (1998) 5648–5652.
[34] C. Lee, W. Yang, R.G. Parr, Development of the Colle-Salvetti correlation-energy formula into a functional of the electron density, Phys. Rev. B Condens. Matter 37 (1988) 785–789.
[35] M.J. Frisch, G.W. Trucks, H.B. Schlegel, G.E. Scuseria, M.A. Robb, J.R. Cheeseman, G. Scalmani, V. Barone, B. Mennucci, G.A. Petersson, H. Nakatsuji, M. Caricato, X. Li, H.P. Hratchian, A.F. Izmaylov, J. Bloino, G. Zheng, J.L. Sonnenberg, M. Hada, M. Ehara, K. Toyota, R. Fukuda, J. Hasegawa, M. Ishida, T. Nakajima, Y. Honda, O. Kitao, H. Nakai, T. Vreven, J.A. Montgomery Jr., J.E. Peralta, F. Ogliaro, M. Bearpark, J.J. Heyd, E. Brothers, K.N. Kudin, V.N. Staroverov, R. Kobayashi, J. Nor-mand, K. Raghavachari, A. Rendell, J.C. Burant, S.S. Iyengar, J. Tomasi, M. Cossi, N. Rega, J.M. Millam, M. Klene, J.E. Knox, J.B. Cross, V. Bakken, C. Adamo, J. Jaramillo, R. Gomperts, R.E. Stratmann, O. Yazyev, A.J. Austin, R. Cammi, C. Pomelli, J.W. Ochterski, R.L. Martin, K. Morokuma, V.G. Zakrzewski, G.A. Voth, P. Salvador, J.J. Dannenberg, S. Da rich, A.D. Daniels, O. Farkas, J.B. Foresman, J.V. Ortiz, J. Cioslowski, D.J. Fox, Gaussian 09, Revision A.02, Gaussian, Inc., Wallingford, CT, 2009.
[36] F. Blanco, I. Alkorta, J. Elguero, Spectral assignments and reference data, Magn. Reson. Chem. 45 (2007) 797–800, https://doi.org/10.1002/mrc.2053.
[37] A.M.S. Silva, R.M.S. Sousa, M.L. Jimeno, F. Blanco, I. Alkorta, J. Elguero, Experimental measurements and theoretical calculations of the chemical shifts and coupling constants of three azines (benzalazine, acetophenoneazine and cinnamaldazine), Magn. Reson. Chem. 46 (2008) 859–864, https://doi.org/10.1002/mrc.2272.
[38] J. Toasi, B. Mennucci, R. Cammi, Quantum mechanical continuum salvation models, Chem. Rev. 105 (2005) 2999–3093.
[39] N. Ozbek, S. Mamaş, T. Erdoğdu, S. Alyar, K. Kaya, N. Karacan, Synthesis, characterization, DFT studies of piperazine derivatives and its Ni(II), Cu(II) complexes as antimicrobial agents and glutathione reductase inhibitors, J. Mol. Struct. 1171 (2018) 834–842.
[40] A.B. Gündüzalp, N. Ozbek, N. Karacan, Synthesis, characterization, and antibacterial activity of the ligands including thiophene/furan ring systems and their Cu(II), Zn(II) complexes, Med. Chem. Res. 21 (2012) 3435–3444.
[41] N. Özbek, S. Alyar, H. Alyar, E. Sahin, N. Karacan, Synthesis, characterization and anti-microbial evaluation of Cu(II), Ni(II), Pt(II) and Pd(II) sulfonylhydrazone complexes; 2D-QSAR analysis of Ni(II) complexes of sulfonylhydrazone derivativesSpectrochim, Acta Mol. Biomol. Spectrosc 108 (2013) 123–132.
[42] H. Alyar, S. Alyar, A. Ünal, N. Özbek, E. Sahin, N. Karacan, Synthesis, characterization and antimicrobial activity of m-toluenesulfonamide, N,N'-1,2-ethanediylbis (mtsen) and [Cu(II)(phenanthroline)2]mtsen complex, J. Mol. Struct. 1028 (2012) 116–125.
[43] U.O. Ozdemir, N. Akkaya, N. Ozbek, New Ni(II), Pd(II), Pt(II) complexes with aromatic methanesulfonylhydrazone based ligands. Synthesis, spectroscopic characterization and in vitro antibacterial evaluation, Inorg. Chim. Acta 400 (2013) 13–19.
[44] G. Ayyannan, M. Mohanraj, G. Raja, N. Bhuvanesh, R. Nandhakumar, C. Jayabalakrishnan, Design, synthesis, structure and biological evaluation of new palladium(II) hydrazone complexes, Inorg. Chim. Acta 453 (2016) 562–573.
[45] S. Sert, O.S. Sentürk, Ü. Ozdemir, N. Karacan, F. Ugur, Synthesis and characterization of the products from reaction of metal carbonyls [M(CO)(6) (M= Cr,Mo, W), Re(CO)(5)Br, Mn(CO)(3)Cp] with salicylaldehyde methanesulfonylhydrazone, J. Coord. Chem. 57 (2004) 183–188.
[46] M. Gaber, M.K. Awad, F.M. Atlam, Pd (II) complexes of bidentate chalcone ligands: synthesis, spectral, thermal, antitumor, antioxidant, antimicrobial, DFT and SAR studies, J. Mol. Struct. 1160 (2018) 348–359.
[47] M. Gaber, H.A. El-Ghamry, M.A. Mansour, Pd(II) and Pt(II) chalcone complexes. Synthesis, spectral characterization, molecular modeling, biomolecular docking, antimicrobial and antitumor activities, J. Photochem. Photobiol. A Chem. 354 (2018) 163–174.
[48] G. Velraj, S. Soundharam, Structure, vibrational, electronic, NBO and NMR analyses of 4-amino-N-[2-pyridinyl] benzene sulfonamide (sulfapyridine) by experimental and theoretical approach, J. Mol. Struct. 1074 (2014) 475–486.
[49] I. Fleming, Frontier Orbitals and Organic Chemical Reactions, Wiley, London, 1976.
[50] T. Koopmans, Über die Zuordnung von Wellenfunktionen und Eigenwerten zu den Einzelnen Elektronen Eines Atoms, Physica 1 (1934) 104–113.
[51] W. Al Zoubi, A.A. Salih, A. Hamdani, S.D. Ahmed, Y. Gun Ko, A new azo-Schiff base: synthesis, characterization, biological activity and theoretical studies of its complexes, Appl. Organomet. Chem. 32 (2018) 3895–3910.
[52] S.M. Abd El-Hamid, S.A. Sadeek, W.A. Zordok, W.H. El-Shwiniy, Synthesis, spectroscopic studies, DFT calculations, cytotoxicity and antimicrobial activity of some metal complexes with ofloxacin and 2,20-bipyridine, J. Mol. Struct. 1176 (2019) 422–433.